

STRAIN HARDENING UNDER NON-PROPORTIONAL LOADING IN POLYCRYSTALLINE ALUMINUM ALLOYS

W. O s i p i u k, K. Ł u k a s z e w i c z

Białystok Technical University
Wiejska 45 C, 15-351 Białystok, Poland

In the paper it is postulated that the so-called common slip domains influence the character of the strain hardening phenomena for complex loading paths. The slip domains were evaluated on the basis of the Batdorf-Budiansky slip theory of plasticity. Evolution of a yield surface for different non-proportional tension-torsion loading paths was determined for PA4 aluminum alloy and the hypothesis that the strain hardening depends on the development of the common slip domains was shown to be justified.

1. INTRODUCTION

Investigations of material behavior under non-proportional loading are of fundamental importance for verification and improvement of the theories of non-elastic deformation and creep. Such investigations can provide a deeper insight into the material deformation mechanisms and thus contribute to improvement of the constitutive equations and the related principal theorems concerning solution uniqueness. One of the most significant phenomena occurring during loading of the common structural materials is strain hardening. Unfortunately, the mechanisms underlying the strain hardening lack a complete understanding, and an adequate and practical theoretical model linking the evolution of the microstructures with the parameters at the macro-scale still remains a challenge.

To approach the strain hardening, various phenomenological models have been introduced and the literature does not provide any consistent view on the hardening phenomena. While some references state that the strain hardening is basically of anisotropic (directional) character [1–4], other maintain that in some cases it can be considered isotropic [5]. References [6, 7] indicate the influence of two effects, that is isotropic when depends on the effective strain and anisotropic when it depends on the principal direction of the strain tensor, the isotropic effect being dominant. The reasons behind the different material behavior under different loading conditions have not been satisfactorily explained. The models of strain hardening are, as a rule, of purely phenomenological character and

generally do not consider the underlying phenomena on the micro-structural level.

The goal of the present paper is to try to explain the differences in material behavior observed experimentally on the basis of the concepts of the slip theory of plasticity. The basic ideas of the slip theory have been presented, among others, by [8–13].

It can be observed that researchers of deformable bodies develop theories based on the microstructure of material [14–17] on the one hand, and theories based on models of an ideally homogeneous body representing means of the properties of a polycrystal on the other hand. The theory presented in this paper belongs to the second category.

It is commonly approved that the plastic deformation of a single crystal can be explained by considering the development of crystallographic slips within certain characteristic planes. A polycrystal body consists of a multitude of crystals and grains with different orientations. In a continuum formulation, the total strain can be regarded as a result of an infinite number of slips along all possible slip planes. This is the basic hypothesis of the Batdorf–Budiansky slip theory of plasticity [8]. It is assumed that the non-elastic deformation leads to an increase of the defect density in a material structure within slip bands [18–22]. The defects constitute barriers to further deformation and the resolved shear stress necessary for continued slip becomes greater. The overall effect is an increase of the macroscopic yield stress and is referred to as strain hardening. Therefore it seems to be justified to formulate a hypothesis that the strain hardening can be described in terms of the slip theory.

Analysis of evolution of the yield surfaces under non-proportional loading is of particular importance for understanding of the basic features of material hardening. Here it is postulated that for complex loading paths, the character of strain hardening is influenced by the so-called common slip domains. The main objective of the present work has been to verify the above hypothesis experimentally. To this aim, yield surfaces for different non-proportional loading paths have been determined. The experiments have been carried out using thin-walled tubular samples of PA4 aluminum alloy subjected to tension and torsion. The slip domains have been evaluated on the basis of the modified Batdorf–Budiansky slip theory [23, 24].

It should be emphasized that a number of researchers [9, 25] propose models which are set in the micromechanics of non-elastic deformation to a much larger degree than the model presented in this work. Such models are very complicated mathematically. The model presented in this work is phenomenological to a large extent and relatively simple, as far as the mathematical side is concerned.

2. THEORETICAL CONSIDERATIONS

The Batdorf–Budiansky slip theory assumes that the material is initially isotropic, i.e. that the spatial arrangement of crystals is disordered and that no direction appears to be privileged. A material body is presumed to be composed of an infinite number of crystals (continuum approach). Possible slip planes within an infinitesimal material volume can be visualized as planes tangent to a half-sphere of a unit radius, any such plane being defined by a normal n given by two angles α and β (Fig. 1).

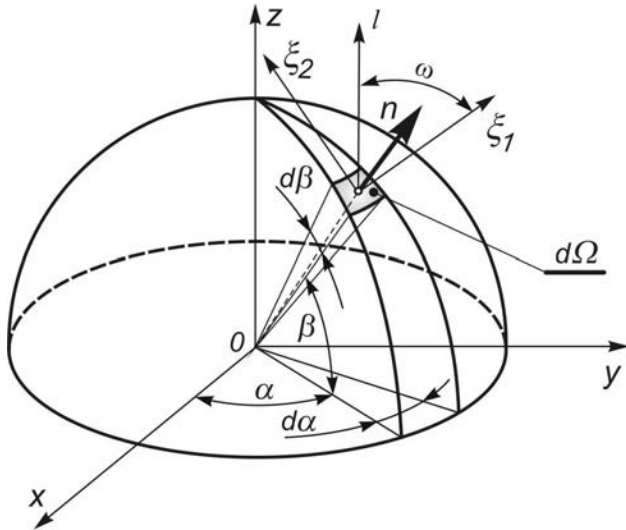


FIG. 1. Half-sphere of unit radius with angles α , β and ω defining the slip planes and slip directions.

The slip direction l within a given slip plane is defined by an angle ω measured from the parallel of latitude axis ξ_1 in the local orthogonal coordinate system (n, ξ_1, ξ_2) (Fig. 1). For all possible slips defined in the n, l system there should be:

$$0 \leq \alpha \leq 2\pi, \quad 0 \leq \beta \leq \pi/2, \quad 0 \leq \omega \leq 2\pi.$$

Among all possible slip systems at a given material point under a given stress state, only some (but possibly infinitely many) will be active. The region on the unit half-sphere corresponding to all slip planes with active slip systems will be here referred to as a slip domain.

By using the tensor transformation rules, the tangent stresses τ in the local coordinates (n, l) can be expressed as follows:

$$(2.1) \quad \tau = \sigma_{ij} l_i n_j \quad (i, j = x, y, z),$$

where σ_{ij} are the stress components in the Cartesian coordinates and n_j and l_i are direction cosines of n and l with respect to the Cartesian coordinates defined as it follows:

$$(2.2) \quad \begin{aligned} l_x &= -\sin \alpha \cos \omega - \cos \alpha \sin \beta \sin \omega, \\ l_y &= \cos \alpha \cos \omega - \sin \alpha \sin \beta \sin \omega, \\ l_z &= \cos \beta \sin \omega, \\ n_x &= \cos \alpha \cos \beta, \quad n_y = \sin \alpha \cos \beta, \quad n_z = \sin \beta. \end{aligned}$$

The total deformation can be calculated by summing up the effects of all active slip systems, namely:

$$(2.3) \quad \gamma_{ij} = \iint_{\Omega} \int_{\omega_1}^{\omega_2} (n_i l_j + n_j l_i) \varphi d\omega d\Omega \quad (i, j = x, y, z),$$

where Ω is the surface area of the half-sphere corresponding to active slip systems, $d\Omega = \cos \beta d\alpha d\beta$, ω_1 and ω_2 are angles bounding the slip directions within the slip planes and φ is the slip intensity function [8].

Here some modifications to the slip theory will be introduced and the slip intensity function φ as proposed by BATDORF and BUDIANSKY [8] will not be used. A function of resistance to plastic deformation S is introduced as follows:

$$(2.4) \quad S = \tau_0 (1 + r\varphi),$$

where τ_0 denotes the yield stress under pure shear, i.e. the initial resistance to plastic deformation (for $\varphi = 0$) and r is a material constant.

It is assumed that the slip system defined by n and l that develops at a given point of a polycrystal body, results in strain hardening mainly in the same system. It also influences hardening in other slip systems. The slip intensity function φ defined with indexes in the system determined by n and l satisfies the condition $\varphi_{n-l} = \varphi_{nl}$. When the sign of external loading is changed, there is an additional term with the minus sign in the function of resistance to plastic deformation S (2.4) (the value of the function S will decrease). Such an approach makes it possible to describe the Bauschinger's effect [23] among other things. The function of resistance to plastic deformation S applied according to the procedure presented below makes it possible to describe the strain-stress curve of the material, e.g. subject to tension.

Function (2.4) being essentially a phenomenological description of a homogeneous model, accounts for the above fundamental feature of strain hardening observed in experimental investigations of elementary slip processes.

A constitutive law for the plastic resistance of an actual material body could be possibly formulated on the basis of the solid-state physics and mathematical statistics. However, the problem is very complicated and thus a simplified description based on function (2.4) is used here.

For material points within regions where slipping occurs one can write:

$$(2.5) \quad \tau = S,$$

while outside of the above regions (i.e. at material points where there is no slipping):

$$(2.6) \quad \tau < S.$$

The variant of the slip theory used in the present work is based on the relations (2.2)–(2.6). The above relations will be now used to evaluate the characteristics of the strain-hardening phenomena with a particular application to such materials as PA4 aluminum alloy. It can be stated that strain hardening develops in material regions where slipping occurs. The above assumption leads to the following hypothesis: Plastic deformation resulting under a certain load state will influence the deformation under subsequently applied other load state, provided that the slip systems generated under the later load state are influenced by the slip systems developed under the former load state. Whether or not, the case can be judged by inspecting the existence of common slip domains on the unit half-sphere for both loading states.

Let us evaluate the slip domains, first in the case of a specimen subjected to the tensile stress σ_z above the yield point, and then in the case of a specimen subjected to the shear stress τ_{xz} resulting from the torsional moment.

On the basis of Eqs. (2.1) and (2.2), the shear stress τ defined in the system n, l on the half-sphere and resulting from σ_z will have the form:

$$(2.7) \quad \tau(\sigma_z) = \frac{1}{2} \sigma_z \sin 2\beta \sin \omega.$$

In order to evaluate the slip intensity function φ , in the system n, l we need to use Eqs. (2.4), (2.5) and (2.7). Then we will obtain:

$$(2.8) \quad r\varphi(\sigma_z) = \frac{\sigma_z}{2\tau_0} \sin 2\beta \sin \omega - 1.$$

As at the slip boundary $\varphi = 0$, the slip domain can be determined by requiring the expression on the right-hand side of Eq. (2.8) to be zero. It can be easily done using numerical methods.

The plastic deformation ε_z is assigned from Eq. (2.3) after replacing the slip intensity function φ by Eq. (2.8).

In the case of the shear stress τ_{xz} resulting from torsional moment, a procedure of evaluating of the slip domain is similar. On the basis of Eqs. (2.1) and (2.2) the shear stress in the system n, l will be expressed by the form:

$$(2.9) \quad \tau(\tau_{xz}) = \tau_{xz} (\cos \alpha \cos 2\beta \sin \omega - \sin \alpha \sin \beta \cos \omega).$$

After using Eqs. (2.4), (2.5) and (2.9), the slip intensity function will take the form:

$$(2.10) \quad r\varphi(\tau_{xz}) = \frac{\tau_{xz}}{\tau_0} (\cos \alpha \cos 2\beta \sin \omega - \sin \alpha \sin \beta \cos \omega) - 1.$$

The plastic deformation γ_{xz} is assigned from Eq. (2.3) after replacing the slip intensity function φ by Eq. (2.10).

In the case of the concurrent action of tensile force and torsional moment on the basis of Eqs. (2.1) and (2.2), the shear stress in the system n, l will be expressed by the form:

$$(2.11) \quad \tau(\sigma_z, \tau_{xz}) = \frac{1}{2} \sigma_z \sin 2\beta \sin \omega + \tau_{xz} (\cos \alpha \cos 2\beta \sin \omega - \sin \alpha \sin \beta \cos \omega).$$

The slip intensity function φ in the system n, l is assigned on the basis of Eqs. (2.4), (2.5) and (2.11), namely:

$$(2.12) \quad r\varphi(\sigma_z, \tau_{xz}) = \frac{1}{\tau_0} \left[\frac{1}{2} \sigma_z \sin 2\beta \sin \omega + \tau_{xz} (\cos \alpha \cos 2\beta \sin \omega - \sin \alpha \sin \beta \cos \omega) \right] - 1.$$

Equation (2.12), after placing it in Eq. (2.3), is used to determine the plastic deformation resulting from the action of a complex load (tension with torsion).

Rigorous analytical calculation of plastic deformation in the case of complex loading is difficult. This concerns the determination of the boundaries of the slip domains and the evaluation of the function (2.3). The above problem can, however, be easily solved by numerical methods. To this aim the half-sphere of unit radius is divided into a great number h of sufficiently small elementary regions denoted by index k

$$(2.13) \quad \Delta\Omega_k = \cos \beta_k \Delta\beta \Delta\alpha,$$

where $\Delta\beta \Delta\alpha$ are the finite intervals of the angles β and α .

The integrals in Eq. (2.3) are approximated by a sum. The plastic deformation conditioned by slips occurring on the elementary k -th region $\Delta\Omega_k$, will be expressed by the forms:

$$(2.14) \quad (\varepsilon_z)_k = \frac{1}{2} \sin 2\beta_k \cos \beta_k \Delta\beta \Delta\alpha \left[\sum_{p=1}^g \sin \omega_p (\varphi_k)_p \Delta\omega \right]_k,$$

$$(2.15) \quad (\gamma_{xz})_k = \cos \alpha_k \cos \beta_k \cos 2\beta_k \Delta\beta \Delta\alpha \left[\sum_{p=1}^g \sin \omega_p (\varphi_k)_p \Delta\omega \right]_k - \frac{1}{2} \sin \alpha_k \sin 2\beta_k \Delta\beta \Delta\alpha \left[\sum_{p=1}^g \cos \omega_p (\varphi_k)_p \Delta\omega \right]_k,$$

where index $p = 1, 2, 3 \dots g$ at ω denotes successive slip directions within the plane n bounded by the angles ω_1 and ω_2 ; $\Delta\omega$ is the value of the finite interval of the angle ω .

According to Eqs. (2.14) and (2.15), the calculations are performed for all elementary regions $\Delta\Omega_k$ forming the surface of the half-sphere. The results are summed, i.e.:

$$(2.16) \quad \varepsilon_z = \sum_{k=1}^h (\varepsilon_z)_k,$$

$$(2.17) \quad \gamma_{xz} = \sum_{k=1}^h (\gamma_{xz})_k,$$

where h denotes the number of elementary regions $\Delta\Omega_k$ occurring within the slips, i.e. $\varphi_k > 0$. If for a given elementary k -th region of the half-sphere the relation $\varphi_k \leq 0$ holds, no slips occur and then in numerical calculation it is assumed that $\varphi_k = 0$. Values of φ_k for next points of the half-sphere are determined on the basis of Eqs. (2.8), (2.9) or (2.12).

The slip domains corresponding to two stress states σ_z and τ_{xz} applied consecutively can either partially overlap or be completely separated. If overlapping occurs then within certain slip planes defined by their normal n , the slipping under shear stresses τ_{xz} will depend on the slips generated under the previously applied normal stresses σ_z . Thus in such a case the strain hardening caused by tensile loading influences the hardening, resulting from a subsequent torsion loading.

Figure 2 and Fig. 3 illustrate the slip domains corresponding to certain values of the stresses σ_z and τ_{xz} . All calculations are performed for $r = 9.3 \cdot 10^3$, $\tau_0 = 105$ MPa, $\Delta\beta = \Delta\alpha = \Delta\omega = 1^\circ$.

If σ_z and τ_{xz} are just above the yield limit, then the slip domains are relatively small and do not overlap, i.e. there is no interaction between the strain hardening caused by the tensile and torsional loads (Fig. 2).

The slip domains for tension and torsion will partially overlap as in Fig. 3, provided the applied stresses are sufficiently large. Those overlapping parts of the slip domains are defined as common slip regions. In that case, predeformation resulting from tension influences the subsequent torsion.

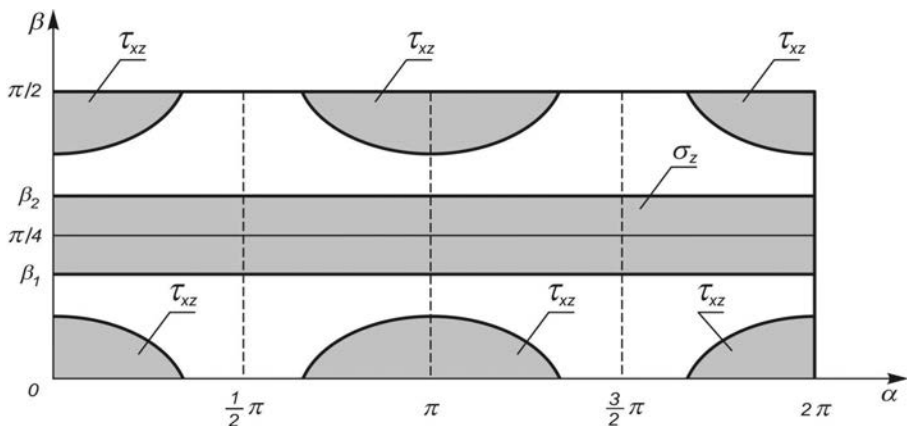


FIG. 2. The slip domains calculated for PA4 aluminum alloy under uni-axial tensile stress state $\sigma_z = 235$ MPa and pure shear stress state $\tau_{xz} = 110$ MPa.

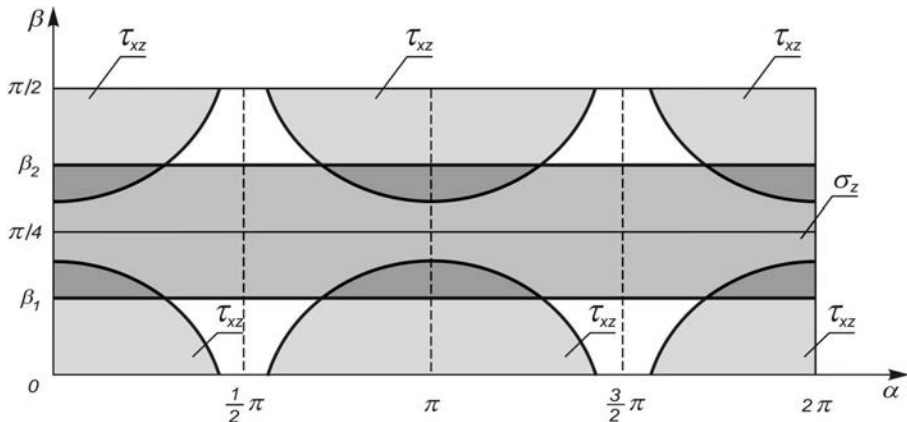


FIG. 3. The slip domains calculated for PA4 aluminum alloy under uni-axial tensile stress state $\sigma_z = 260$ MPa and pure shear stress state $\tau_{xz} = 148$ MPa.

3. EXPERIMENTAL INVESTIGATION

In order to verify the above theoretical considerations, a number of experiments using thin-walled cylindrical samples were carried out on the tension-torsion machine Instron 8502 Plus. The samples were made of aluminum alloy PA4 (containing 0.7–1.2% Mg, 0.6–1.0% Mn, 0.7–1.2% Si, below 0.5% Fe, and impurities of 0.1% Cu and 0.2% Zn). The dimensions of the samples were as follows: the external diameter 17.5 mm, the wall thickness 0.75 mm and the measurement length 75 mm. The samples were subjected to a preliminary homogenizing treatment at a temperature of 438 K for 6 hours. The method de-

scribed in Ref. [26] was used to test for material anisotropy and following the thermal treatment, the mechanical properties were found to be isotropic. The stress-strain curve obtained for tensile loading is shown in Fig. 4. The apparent yield stress under tension was found to be $R_{0.1} = 220.2$ MPa while the elastic modulus was $E = 72319$ MPa. On the basis of the strain-stress curve the initial yield stress has been evaluated $\sigma_0 = 210$ MPa. In that case the initial shear stress is $\tau_0 = 105$ MPa (τ_0 is initial resistance to plastic deformation).

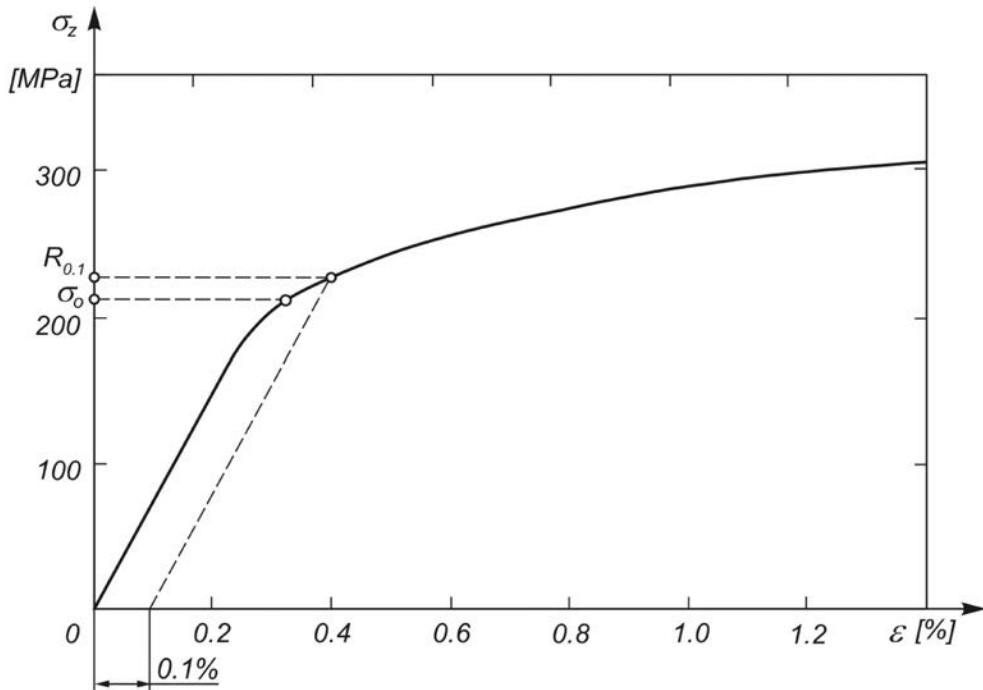


FIG. 4. Stress-strain curve for aluminum alloy: apparent yield stress $R_{0.1} = 220.2$ MPa, initial resistance to plastic deformation $\tau_0 = 105$ MPa.

Two series of experiments were carried out. The samples in the first group were subjected to a tensile force (causing some initial plastic deformation) followed by unloading (partial or complete and different for different samples). Subsequently, a torsional moment was applied and its value was increased from zero up to the point resulting with deformation intensity of 0.1%. The above method based on the apparent yield point (assumed in the present work to represent the yield criterion) proved to be more effective than the Lode extrapolation method, due to a straightforward implementation in the computer program controlling the testing machine. Each loading path was repeated for two samples.

Figure 5 shows the exemplary loading path of the sample that was first subjected to the tensile stress σ_z^B , then unloaded by diminishing stress to the

value σ_z^C , and after that subjected to the shear stress τ_{xz} of the value causing deformation intensity of 0.1%.

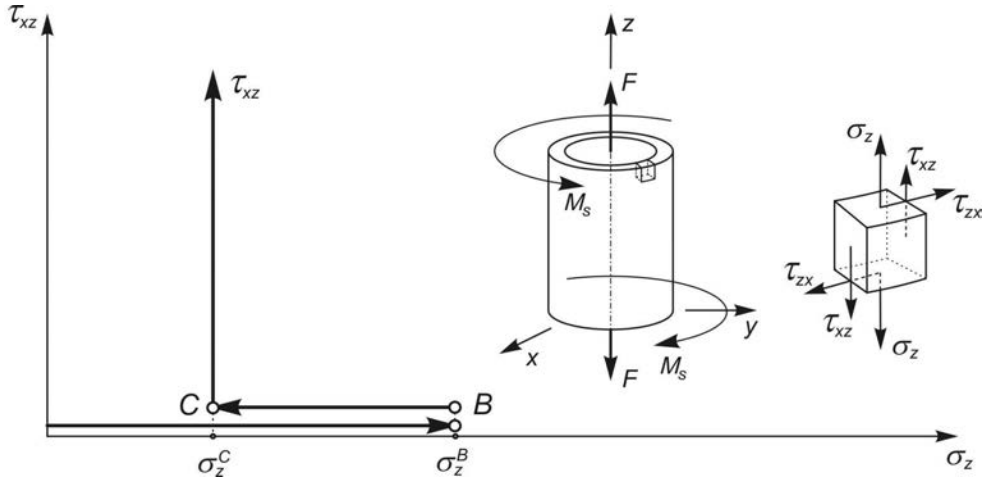


FIG. 5. The exemplary loading path of the sample subjected first to a tensile force and then (after partial unloading) to a torsional moment.

It is observed that as a result of the tensile stresses σ_z^B at the point B , the material slips by $\varphi^B(\sigma_z)$. The value of the slip can be determined on the basis of Eq. (2.8), i.e.:

$$(3.1) \quad r\varphi^B(\sigma_z) = \frac{\sigma_z^B}{2\tau_0} \sin 2\beta \sin \omega - 1.$$

After unloading the sample to the point C and applying a torsional moment resulting with the shear stress τ_{xz} , the plastic resistance function (2.4) will take the form:

$$(3.2) \quad S = \tau_0 [1 + r (\varphi^B + \varphi)],$$

where φ^B denotes the value of the slip intensity function at the point B determined according to (3.1).

It is assumed that plastic deformations do not decay after unloading, i.e. the value of the slip intensity function does not get lower after diminishing tensile stress (strain hardening of a material does not decrease). This being so, on the basis of Eqs. (2.5) and (3.2) the slips condition after partial unloading and subsequent applying the shear stress τ_{xz} will take the following form:

$$(3.3) \quad \tau_0 [1 + r (\varphi^B + \varphi)] = \tau (\sigma_z^C, \tau_{xz}),$$

where the shear stress function $\tau(\sigma_z^C, \tau_{xz})$ in the system n, l is expressed by the relation (2.11) with $\sigma_z^C = \sigma_z^B - \Delta\sigma_z$.

On the basis of the condition (3.3) one will obtain:

$$(3.4) \quad r\varphi = \frac{1}{\tau_0} \tau(\sigma_z^C, \tau_{xz}) - r\varphi^B - 1.$$

The Eq. (3.4) makes it possible to calculate the value of the shear stress τ_{xz} causing the definite plastic deformation in the case when there was a predeformation caused by the tensile stress σ_z^B . The above calculations can be performed using Eqs. (2.11), (2.13)–(2.17), and their results are presented in Fig. 6 as lines a, b, c .

Figure 6 presents graphically the experimental results of strain hardening depending on the loading path. The strain hardening is the cause of the expansion and shift of the plasticity surface, in relation to the initial surface determined for $\varepsilon_i = 0.1\%$.

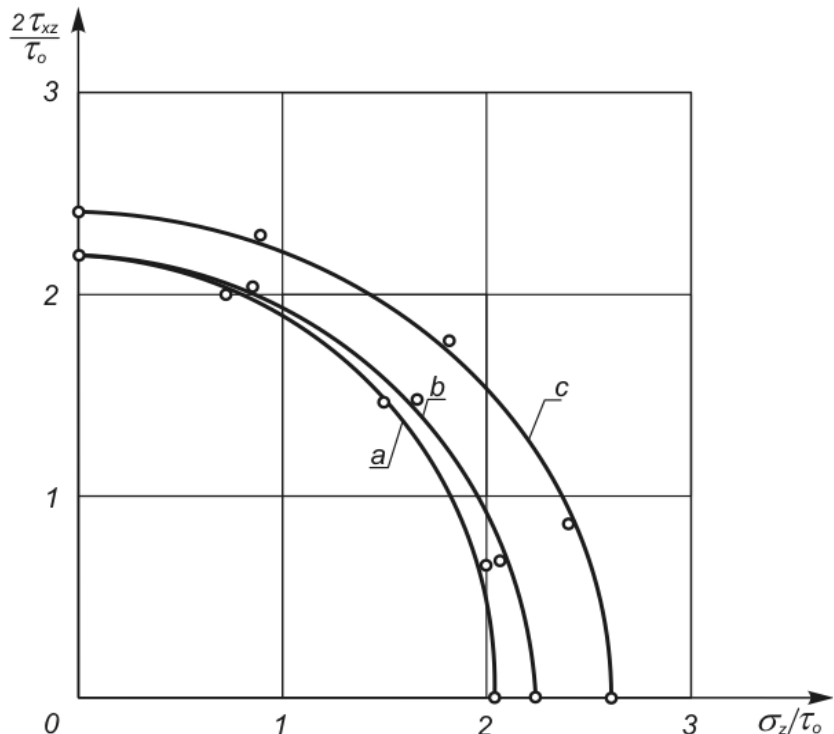


FIG. 6. Evolution of the yield surface for PA4 aluminum alloy determined using thin-walled tubular samples under combined tension and torsion, with initial plastic deformation induced by preliminary tensile loading (a – initial surface; b, c – evolving surfaces for increasing plastic deformation).

4. CONCLUDING REMARKS

Analysis of the experimental results presented in Fig. 6, taking into account the slip domains illustrated in Fig. 2 and Fig. 3, confirms the hypothesis formulated in Sec. 2 of the present paper. The plastic properties of a given material are determined by interaction of the slip systems that develop during loading. At a given material point, the strain hardening corresponding to the plastic deformation under tensile loading influences the subsequent plastic deformation under torsion loading, provided there are common slip domains. The existence of the common slip domains can be verified using the relations presented above.

The case shown in Fig. 2 corresponds to a situation when there is no interaction between the slip systems developed under two consecutively applied stress states. The case is represented by the curves *a* and *b* in Fig. 6. The curve *c* in Fig. 6 corresponds to the location of slip domains as shown in Fig. 3. It can be observed that the slip domains overlap.

The hardening model is found to be a good approximation in cases when plastic deformation is small.

Increasing of plastic deformation causes the common slip domains to grow and thus the yield surface changes not only due to the transformation of its center in the direction of loading but also due to an increase of its size in the transverse directions.

ACKNOWLEDGEMENTS

The research was carried out under the project S/WM/1/07 realized in the Białystok Technical University.

REFERENCES

1. Z. L. KOWALEWSKI, *Creep of metals: experiment and modeling* [in Polish], IPPT PAN, Warszawa 2005.
2. J. LIN, Z. L. KOWALEWSKI, J. CAO, *Creep rupture of copper and aluminium alloy under combined loadings-experiments and their various descriptions*, Int. J. of Mechanical Sciences, **47**, 1038–1058, 2005.
3. F. BARLAT, J. M. FERREIRA DUARTE, J. J. GRACIO, A. B. LOPES, E. F. RAUCH, *Plastic flow for non-monotonic loading conditions of an aluminum alloy sheet sample*, Int. J. of Plasticity, **19**, 1215–1244, 2003.
4. H. P. FEIGENBAUM, Y. F. DAFALIAS, *Directional distortional hardening in metal plasticity within thermodynamics*, Int. J. of Solids and Structures, **44**, 7526–7542, 2007.
5. W. M. MAIR, H. L. D. PUGH, *Effect of prestrain on yield surfaces in copper*, J. Mech. Engg. Sci., **6**, 150–163, 1964.

6. Z. MRÓZ, W. TRĄMPCZYŃSKI, D. R. HAYHURST, *Anisotropic creep hardening rule for metals and its application to cyclic loading*, Int. J. of Plasticity, **4**, 279–299, 1988.
7. Z. MRÓZ, W. TRĄMPCZYŃSKI, *On the creep hardening rule for metals with memory of maximal prestress*, Int. J. Solids Structures, **20**, 467–486, 1984.
8. S. B. BATDORF, B. BUDIANSKY, *A mathematical theory of plasticity based on the concept of slip*, NACA, TN 1871, 1949.
9. P. DŁUŻEWSKI, *Continual theory of dislocations as a theory of constitutive modeling of finite elastic-plastic deformations* [in Polish], IPPT PAN, **13/96**, Warszawa 1996.
10. T. H. LIN, S. G. RIBEIRO, *Development of a physical theory of plasticity*, Int. J. of Solids and Structures, **17**, 545–551, 1981.
11. Y. F. DAFALIAS, *Orientation distribution function in non-affine rotations*, J. Mech. Phys. Solids, **49**, 2493–2516, 2001.
12. M. V. GLAZOFF, F. BARLAT, H. WEILAND, *Continuum physics of phase and defect microstructures: bridging the gap between physical metallurgy and plasticity of aluminum alloys*, Int. J. of Plasticity, **20**, 363–402, 2004.
13. I. S. NIKITIN, *Constitutive equations of the elastoviscoplastic model and slip theory*, Mechanics of Solids, **42**, 260–270, 2007.
14. A. NEEDLEMAN, M. E. GURTIN, *Boundary conditions in small-deformation, single-crystal plasticity that account for the Burgers vector*, J. of Mechanics and Physics of Solids, **53**, 1–31, 2005.
15. G. WINTHON, D. J. JENSEN, N. HANSEN, *Dense dislocation walls and microbands aligned with slip planes – theoretical considerations*, Acta Mater., **45**, 12, 5059–5068, 1997.
16. N. HANSEN, X. HUANG, D. A. HUGHES, *Microstructural evolution and hardening parameters*, Mater. Sci. Eng., **A317**, 3–11, 2001.
17. M. P. ARIZA, M. ORTIZ, *Discrete Crystal Elasticity and Discrete Dislocations in Crystals*, Arch. Rational Mech. Anal., **178**, 149–226, 2005.
18. D. HULL, D. J. BACON, *Introduction to dislocations*, (Fourth Edition), Pergamon Press, Oxford, 2001.
19. J. ADAMCZYK, *Theory of metals – Part 3. Plastic straining, hardening and fracture* [in Polish], Silesian University of Technology, Gliwice, 1993.
20. H. J. FROST, M. F ASHBY, *Deformation – mechanism maps. The plasticity and creep of metals and ceramics*, Pergamon Press, Oxford, 1982.
21. K. PRZYBYŁOWICZ, *Metallurgy* [in Polish], WNT, Warszawa 2003.
22. R. J. ASARO, B. ZHU, P. KRYSL, R. BAILEY, *Transition of deformation mechanisms and its connection to grain size distribution in nanocrystalline metals*, Acta Mater., **53**, 4825–4838, 2005.
23. W. OSIPIUK, *Non-elastic deformation and fracture of metals* [in Polish], Białystok Technical University, 1999.
24. K. N. RUSINKO, *Theory of plasticity and non-stationary creep* [in Russian], Lvov, Visca Skola, 1981.

25. F. MOREL, *A critical plane approach for life prediction of high cycle fatigue under multiaxial variable amplitude loading*, Int. J. of Fatigue, **22**, 101–119, 2000.
26. M. ANISIMOWICZ, *Investigation of vibrocreep of metal alloys under plane stress state* [in Polish], IFTR, IFTR Reports, 1978.

Received November 30, 2005; revised version June 16, 2008.
